Final Report - Photogrammetry Project

Alaska Center for Energy and Power - University of Alaska Fairbanks
Prepared by Logan Borger
August 7, 2020

Overview

The focus of this project has been both the utilization of photogrammetric data captured by unmanned aerial systems (UASs) at various locations to produce digital models for further analysis and the creation of a repeatable workflow of the aforementioned process for the benefit of students and staff at the Alaska Center for Energy and Power (ACEP). This workflow was compliant with the United States Defense Information Systems Agency (DISA) requirements and will allow students and staff to understand and navigate both the theoretical and technical components of executing this type of work. For four sites, digital surface models (DSMs), Digital Terrain Models (DTMs), orthomosaics, and canopy height models (CHMs) were created in order to better understand and interpret variability in the study areas (Remondino, 2011).

Introduction

The science of photogrammetry, which includes utilizing photographs from unmanned aerial systems and processing these into digital surface models and concurrently quantitative measurements, has many applications for both analyzing changes in topography and changes in vegetation (Westoby, 2012). This study is focused on producing DSMs among other products to understand the characteristics of permafrost and coastal erosion processes relevant to energy and power applications.

There are four areas of study in various locations within the state of Alaska. The first two sites are based in Fairbanks, Alaska on long-term permafrost study sites. 1) The first study area is the Permafrost Tunnel Research Facility, which is owned by US Army Garrison Fort Wainwright and operated and maintained by Cold Regions Research and Engineering Laboratory. The site was developed around studying a silt escarpment containing warm, ice-rich, fine-grained permafrost. 2) The second study area is the Permafrost Experiment Station which is owned and operated by the same entities. This site has been heavily modified since 1946 to simulate the effects of construction or similar types of disturbance like forest fires on ice-rich permafrost. 3) The third study area is located just south of Yakutat, which is a small rural community in the Gulf of Alaska that can only be accessed by air and sea. This site faces growing concerns of documented erosion in the area where erosion of beach dunes can lead to saltwater intrusion into local estuaries and changes in landscape structure and function. 4) The fourth study area is Foggy Island Bay, which is located on the north slope adjacent to the Beaufort Sea. This site's data will be focused on bay wave hydrodynamics and sediment transport in relation to prospective projects of Hilcorp.

As with any process, producing models comes with its associated error. For photogrammetry, error can be mitigated by adding ground control points (GCPs), which are used for weaving the

photos together. These GCPs each come with their own individual error, which can impact the overall error of the model. In order to optimize the photogrammetry process it is necessary to minimize the variability and to reduce the error of the produced models as much as possible. This report will encapsulate a moderate exploration of the error associated with GCPs, their impact on models, and provide insight into optimizing the accuracy of future models that are produced. This report will also start to explore the optimization of settings for Classifying Ground Points, which remains a relatively unexplored, yet important step of the photogrammetry process.

Methodology

Photogrammetric data was processed into geospatial models with the use of Agisoft Metashape and python notebooks. Additionally QGIS was used, but predominantly for trial visualizations for future python notebooks; the functionality of QGIS has been generally shifted to python notebooks, which works better for processing larger amounts of data and producing consistent results. This conglomerate of software forms the core of photogrammetry on the cloud.

Following the photogrammetry instructions, iterative testing was conducted, using the workflow in Figure 1, to produce geospatial models with varying inclusion of GCPs. The inclusion of GCPs and the corresponding errors can be found here. Sites were initially processed to contain GCPs with errors less than 0.1 meters, which produced models with less error. These sites were then reprocessed to contain all GCPs, which in turn produced models with the most amount of error. These models were then differenced using this python notebook, which allows us to visualize the impact of GCP error on the geospatial models being produced. Furthermore, difference models, histograms, and hillshades were produced for each of the four sites.

The optimization of the “Ground Point Classification” step in the photogrammetry instructions will also be explored to some extent. Full optimization would take extensive iterative testing for multiple sites. Four iterations of testing will be conducted to produce various digital terrain models. These models will then be differenced and analyzed. A recommendation for future iterations to determine the optimal settings will be made. Exploration of these settings and optimizing them will take time, however these first iterations lay the groundwork for future iterations. Iterations for the classification of ground points were conducted on the Permafrost Tunnel site. This report encompasses some iterations of differing classes for ground point classification.

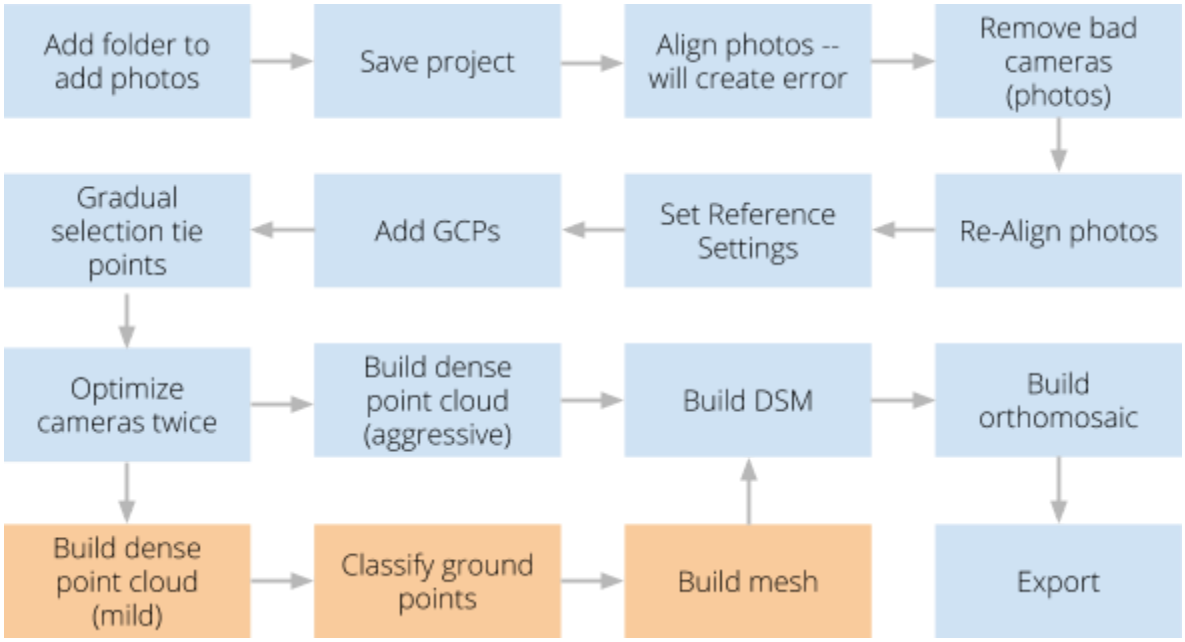

Figure 1: Agisoft Metashape Professional workflow used for this project. Items in blue were completed in the first round of processing while items in orange were repeated as an add-on step in order to produce the digital terrain model (DTM) with only ground points included.

Results

Ground Control Point Error

The iterations of testing GCPs can be found here. It is clear that inclusion of inaccurate GCPs (above 0.1 m) can skew the models produced. Below is the results from differencing models. These figures focus on the error caused by GCP error.

Permafrost Tunnel

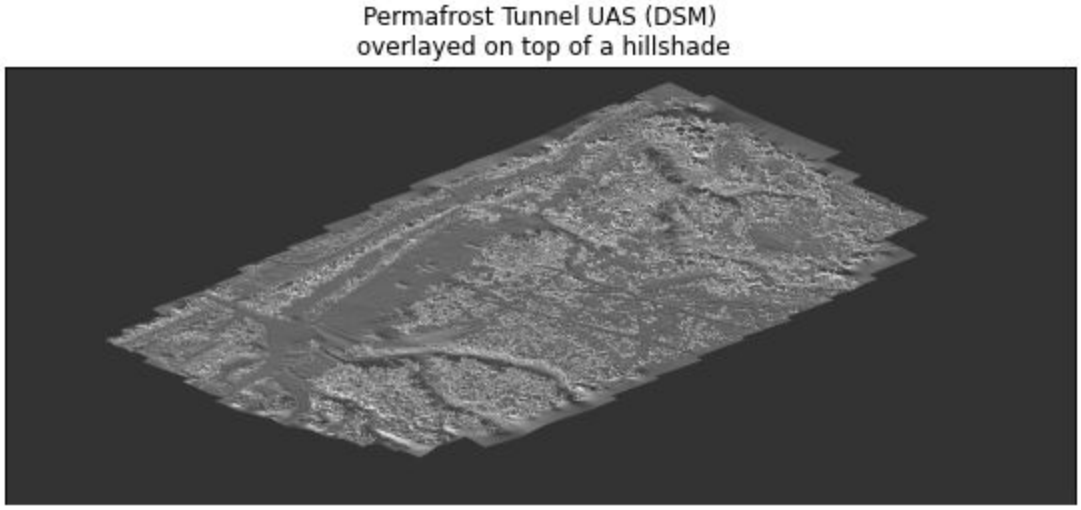

Figure 2: This is a Hillshade model of the Permafrost Tunnel Site. Here it is possible to see the topography of the site.

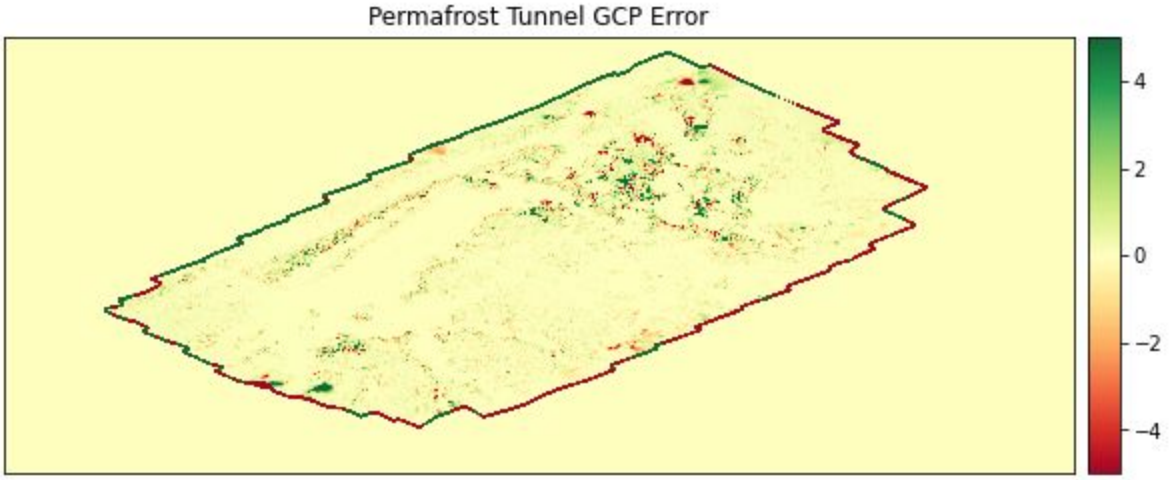

Figure 3: This is a differencing of the most accurate, with GCP accuracy of .059, compared to the least accurate model, with GCP accuracy of .141. This figure shows the difference between these models, which was caused by GCP error. The areas in red illustrate negative elevation changes in the model in meters, while the areas in green illustrate positive elevation changes in meters.

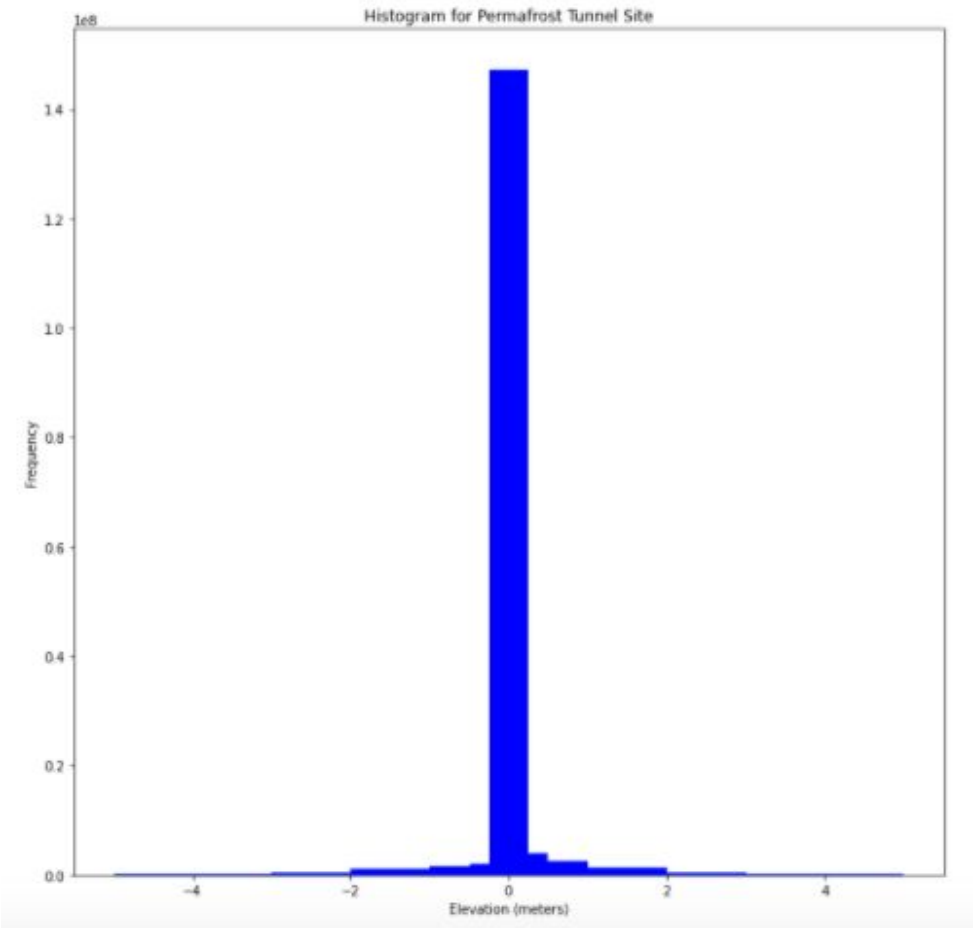

Figure 4: This is a histogram of the Permafrost Tunnel Site. Here it is possible to see the distribution of the error.

Permafrost Station

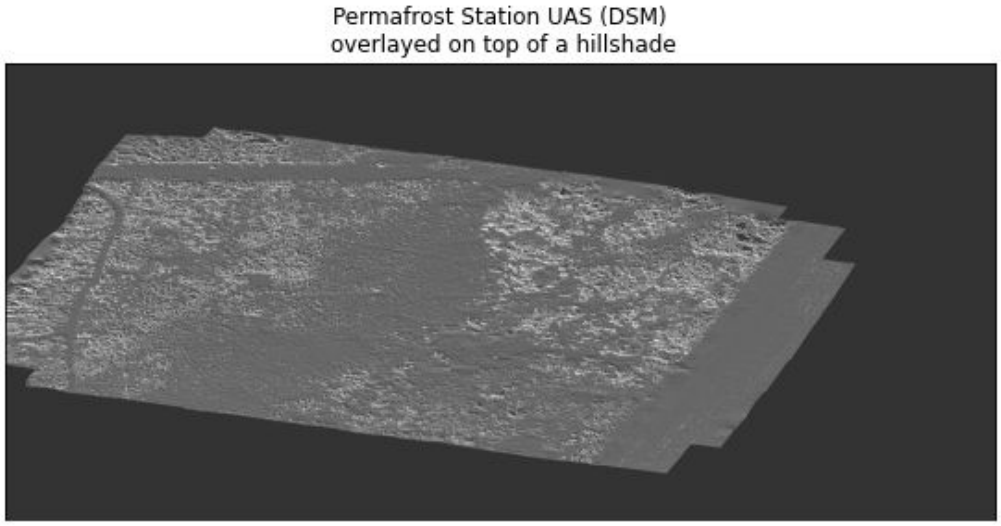

Figure 5: This is a Hillshade model of the Permafrost Station Site. Here it is possible to see the topography of the site.

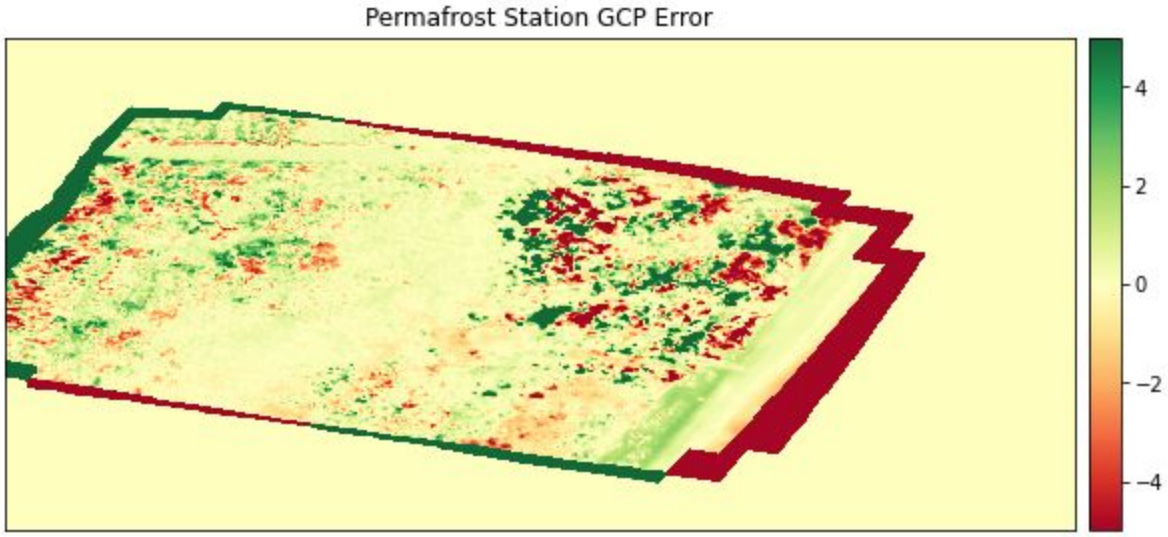

Figure 6: This is a differencing of the most accurate, with GCP accuracy of .053, compared to the least accurate model, with GCP accuracy of 30.365. This figure shows the difference between these models, which was caused by GCP error. The areas in red illustrate negative elevation changes in the model in meters, while the areas in green illustrate positive elevation changes in meters.

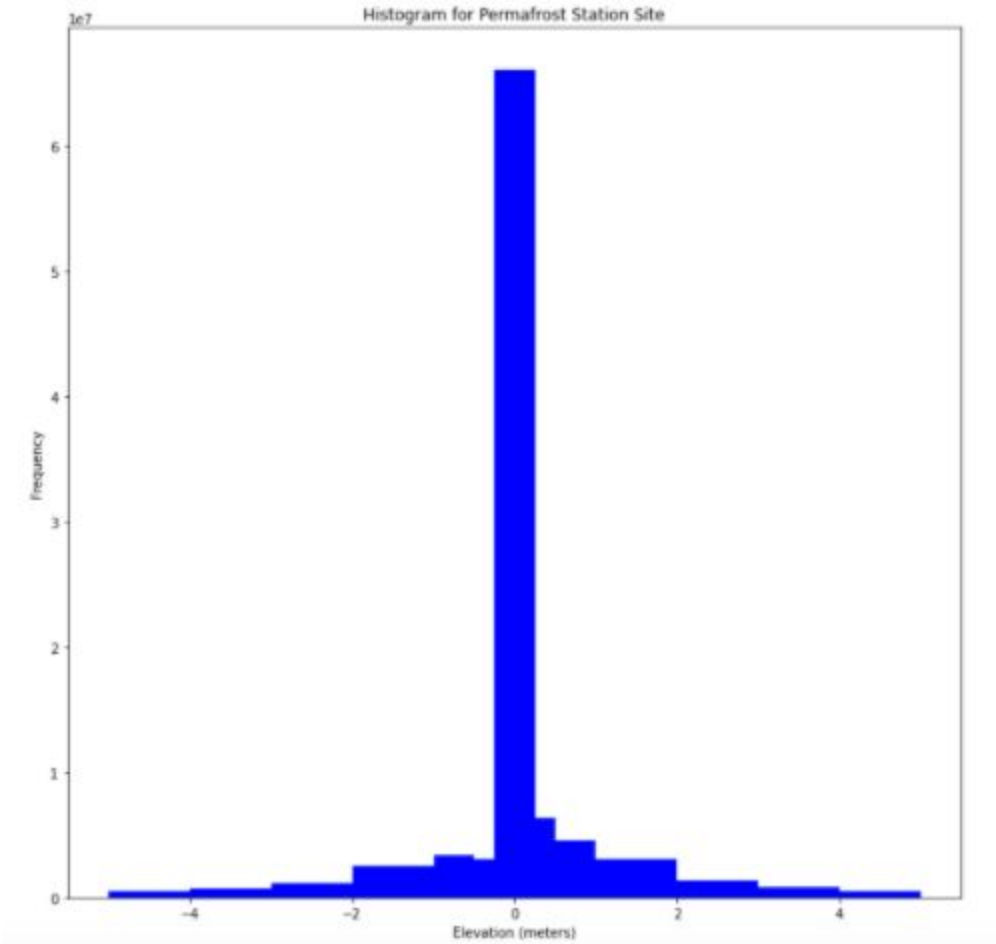

Figure 7: This is a histogram of the Permafrost Station Site. Here it is possible to see the distribution of the error.

Yakutat

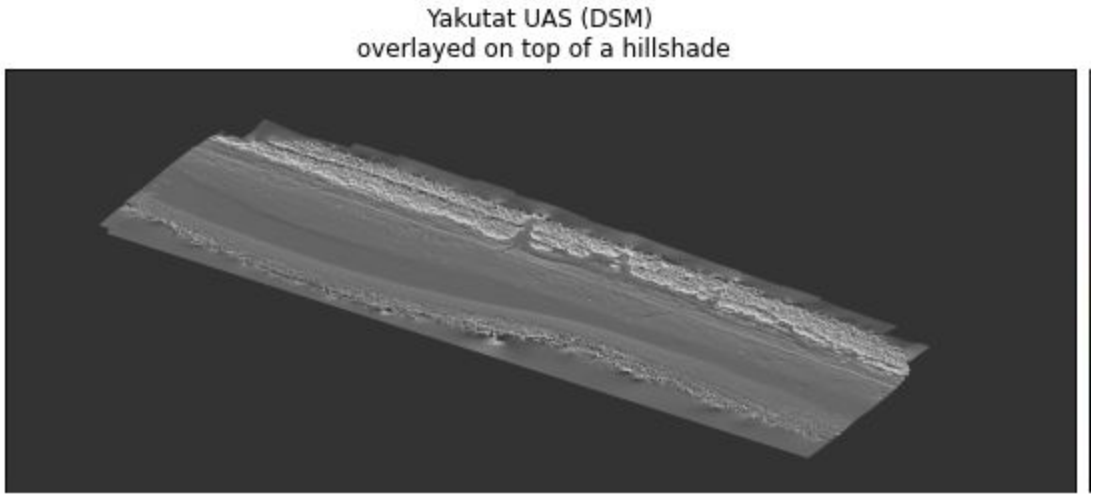

Figure 8: This is a Hillshade model of the Yakutat Site. Here it is possible to see the topography of the site.

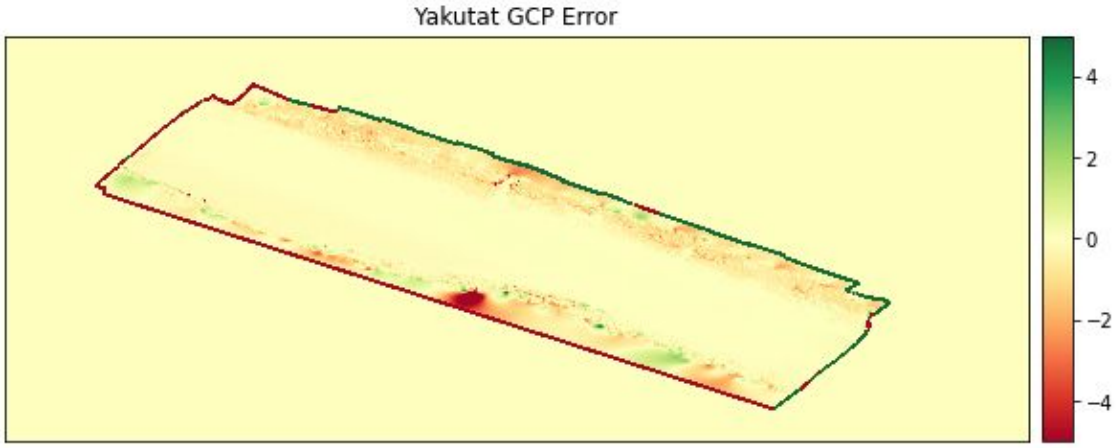

Figure 9: This is a differencing of the most accurate, with GCP accuracy of .055, compared to the least accurate model, with GCP accuracy of .15. This figure shows the difference between these models, which was caused by GCP error. The areas in red illustrate negative elevation changes in the model in meters, while the areas in green illustrate positive elevation changes in meters.

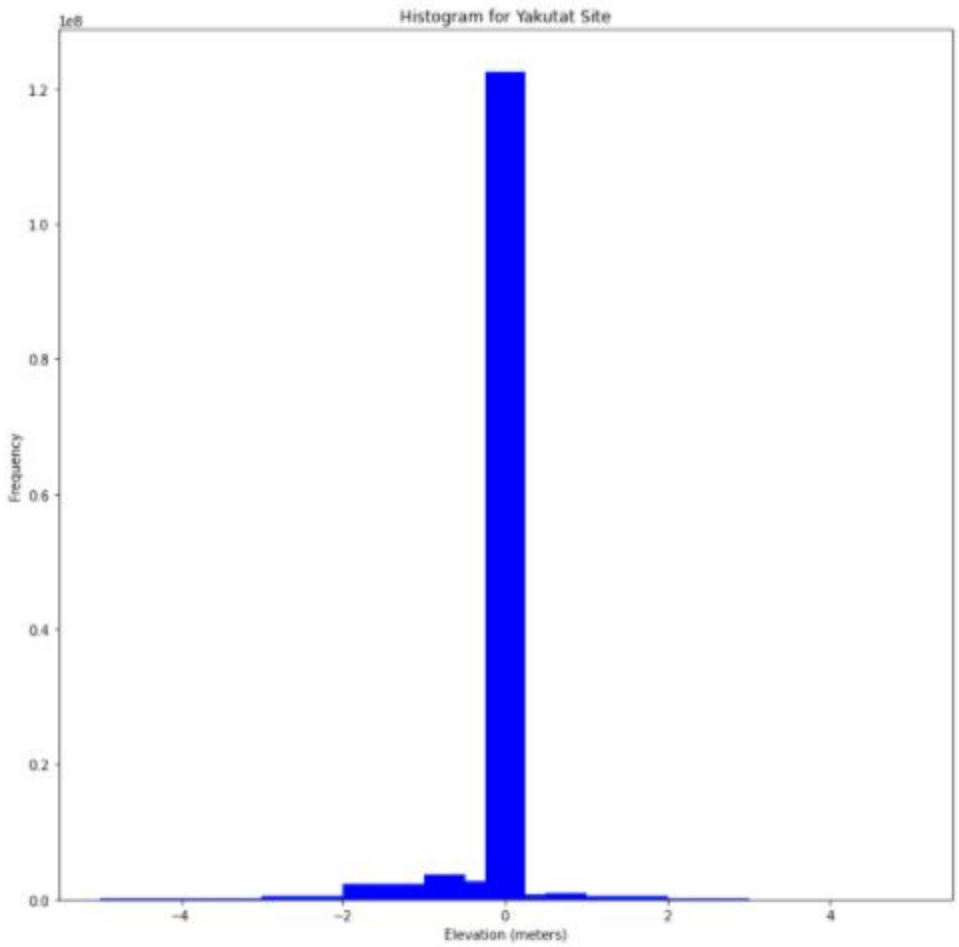

Figure 10: This is a histogram of the Yakutat Site. Here it is possible to see the distribution of the error.

Foggy Island Bay

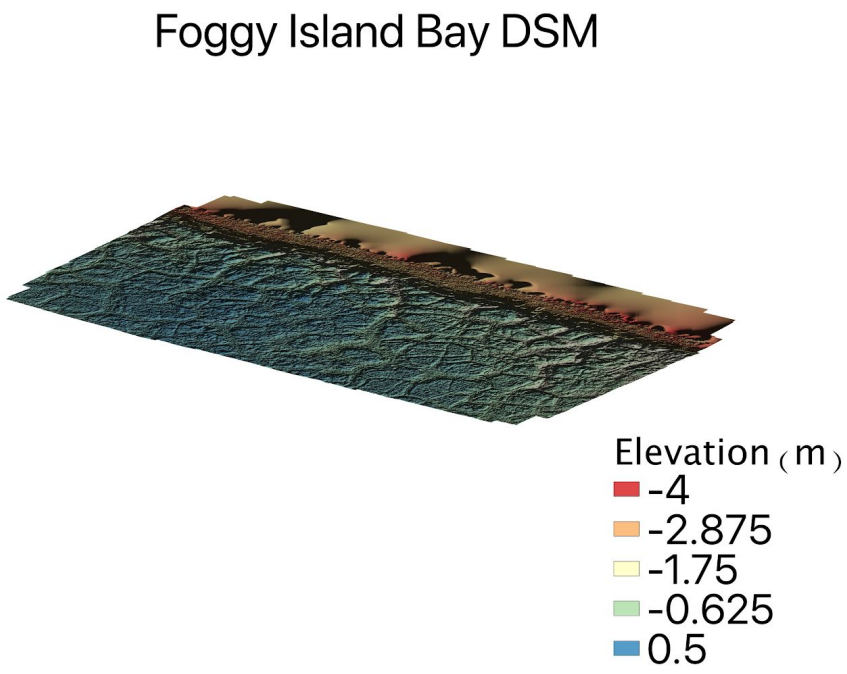

Figure 11: This is a Hillshade model of the Foggy Island Bay Site. Here it is possible to see the topography of the site.

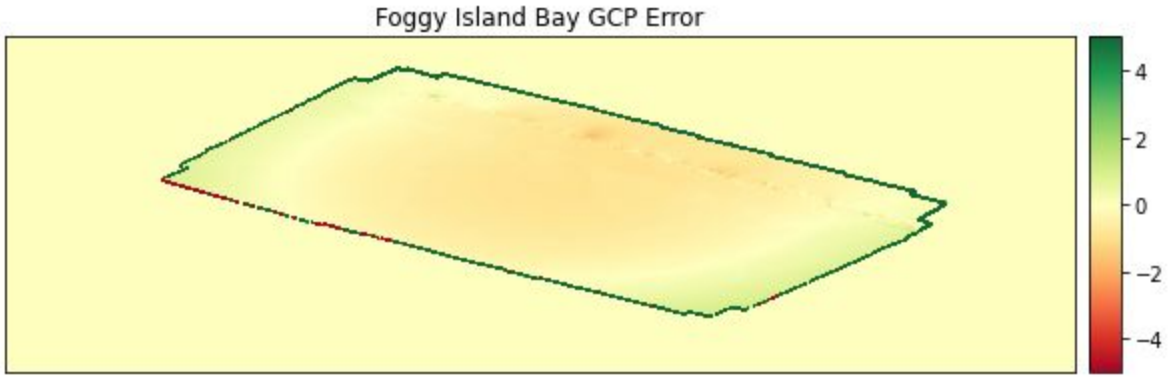

Figure 12: This is a differencing of the most accurate, with GCP accuracy of .06, compared to the least accurate model, with GCP accuracy of .148. This figure shows the difference between these models, which was caused by GCP error. The areas in red illustrate negative elevation changes in the model in meters, while the areas in green illustrate positive elevation changes in meters.

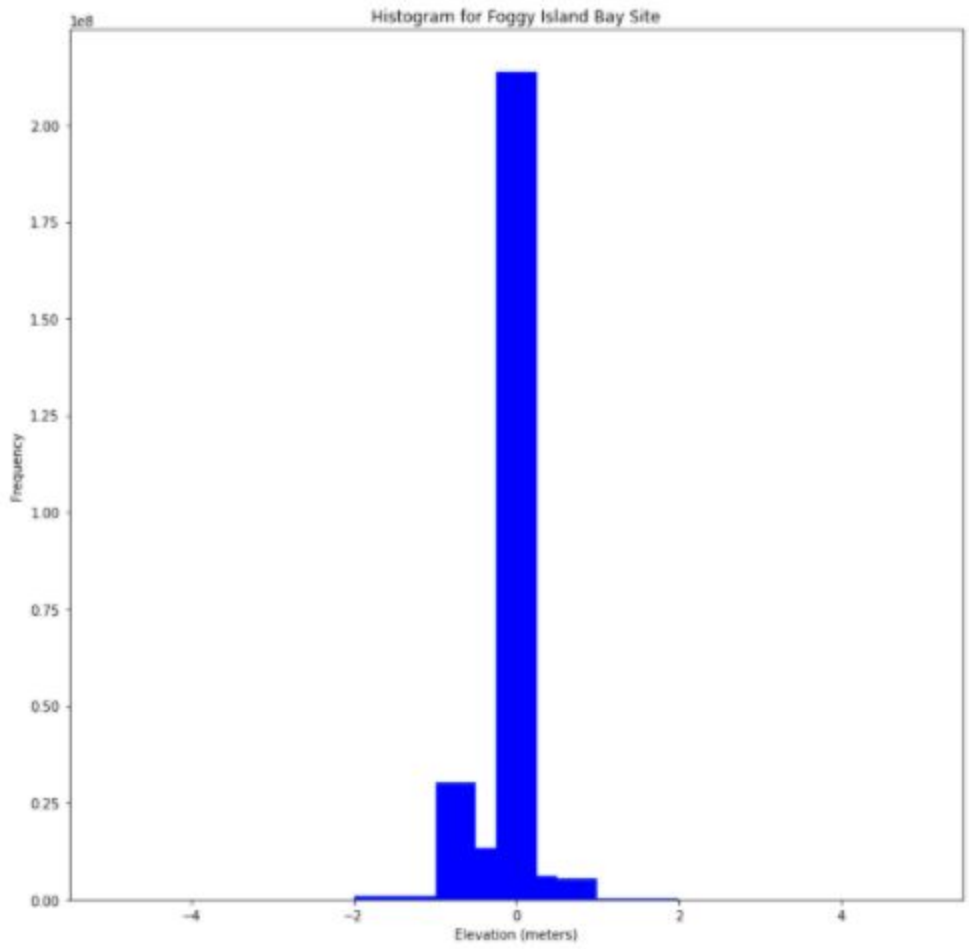

Figure 13: This is a histogram of the Foggy Island Bay Site. Here it is possible to see the distribution of the error.

From these models, it is clear that GCP error impacts the models and creates significant variance. The above figures show the general trend of instances of error between -2 to 2 meters. This should emphasize the importance of not using GCPs with error values above 0.1 meters, especially when conducting precise comparisons.

Classifying Ground Points
Conducted iterations of settings can be found here.

Permafrost Tunnel Iteration 1 - Class: Created (Never Classified)

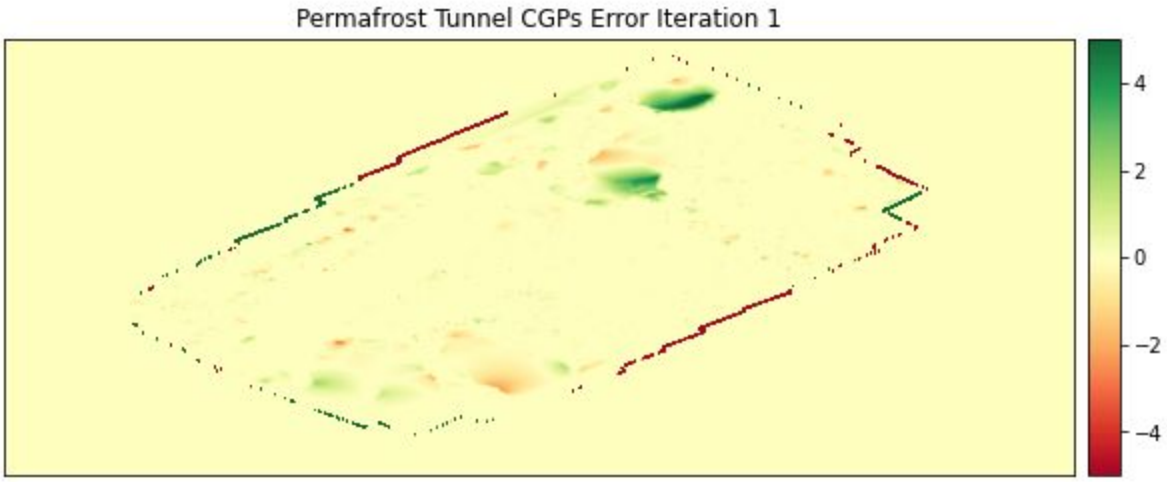

Figure 14: This is a differencing of a digital terrain produced with the ground classification settings "Class: Created (Never Classified)" and the baseline default settings "Class: Any Class". The areas in red illustrate negative elevation changes in the model in meters, while the areas in green illustrate positive elevation changes in meters.

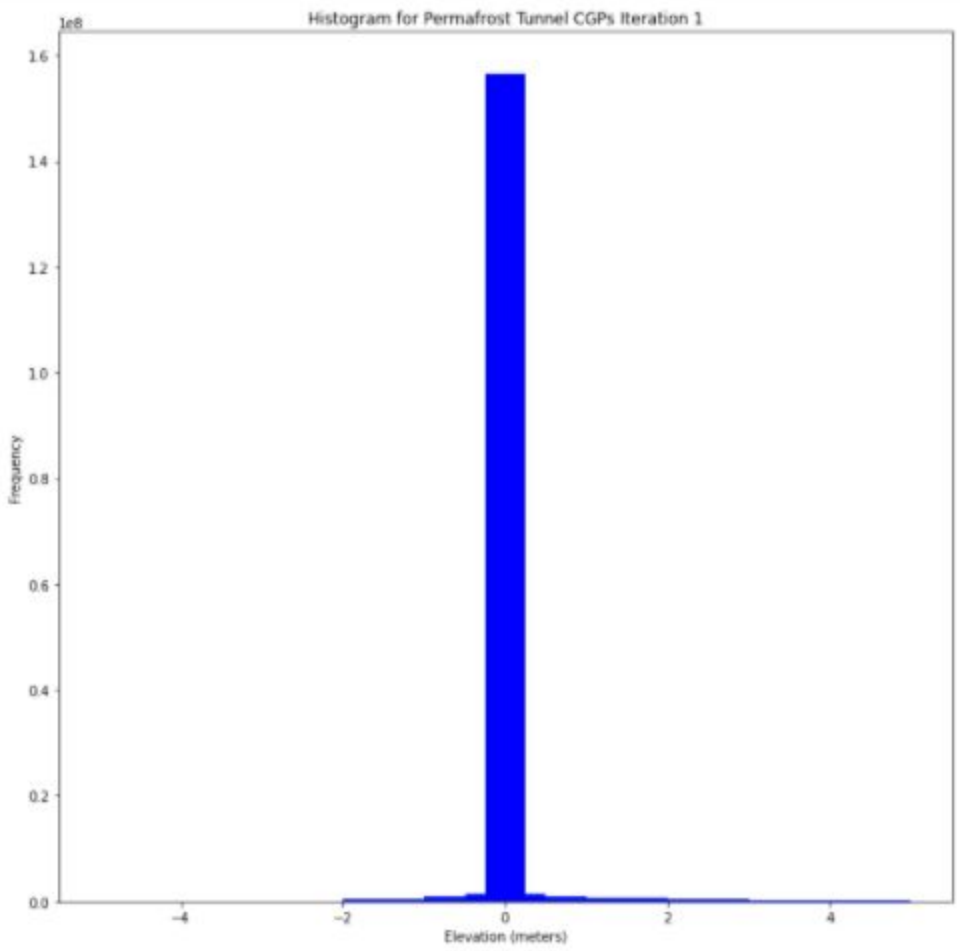

Figure 15: This is a histogram of the Permafrost Tunnel CGPs Iteration 1. Here it is possible to see the distribution of the error.

Permafrost Tunnel Iteration 2 - Class: Unclassified

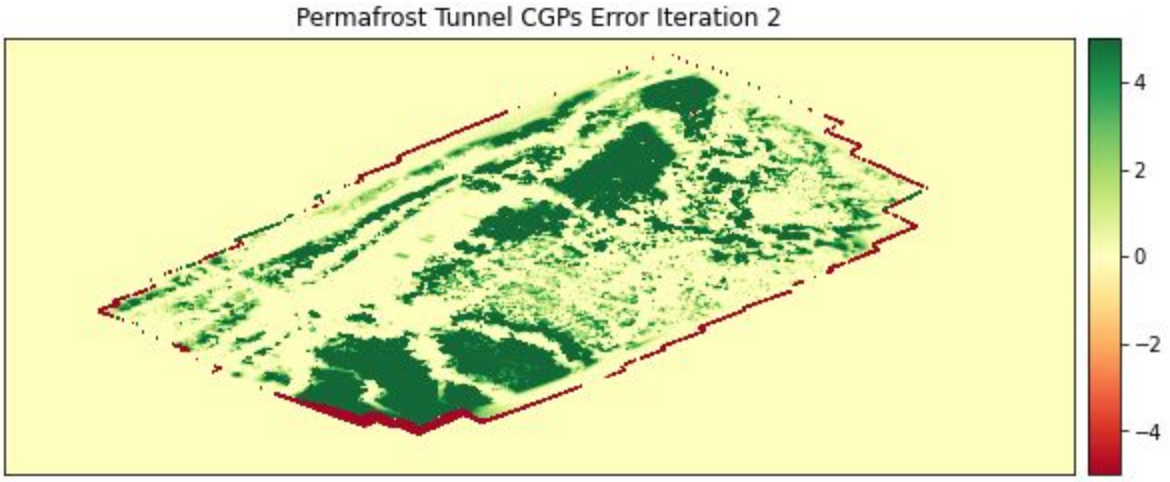

Figure 16: This is a differencing of a digital terrain produced with the ground classification settings “Class: Unclassified” and the baseline default settings “Class: Any Class”. The areas in red illustrate negative elevation changes in the model in meters, while the areas in green illustrate positive elevation changes in meters.

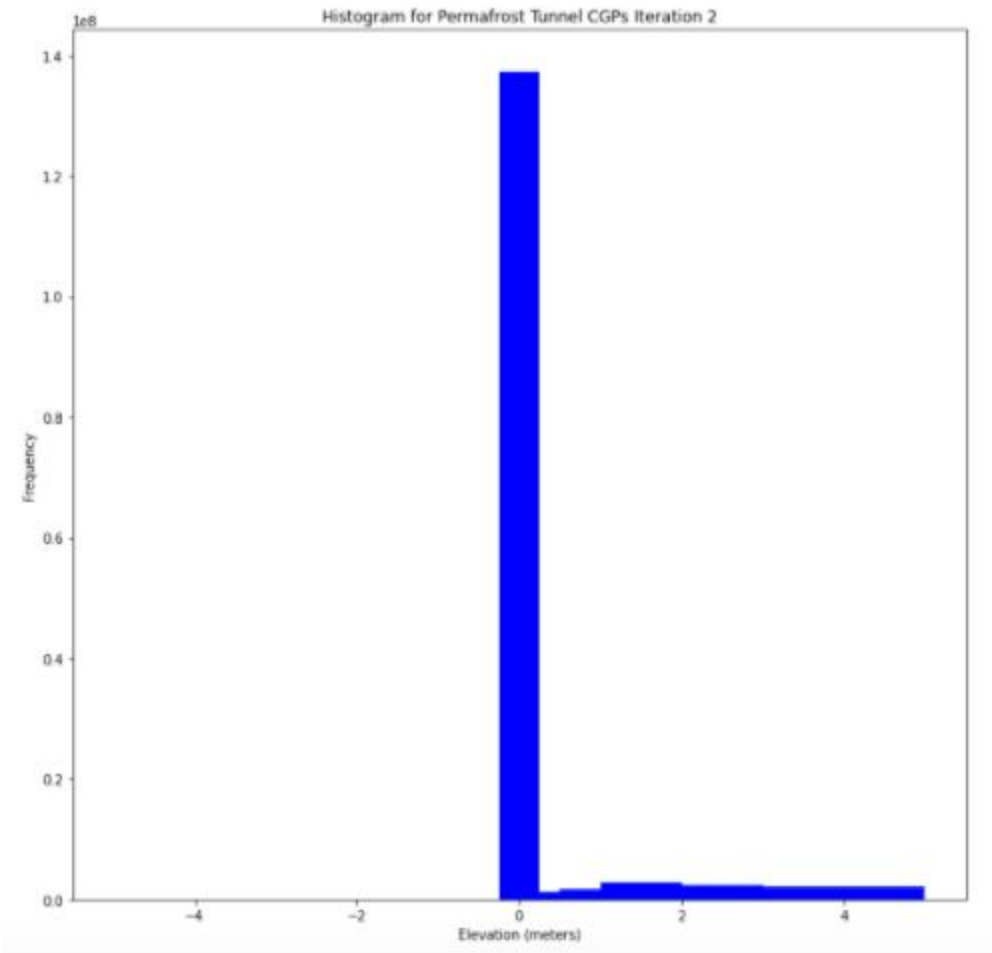

Figure 17: This is a histogram of the Permafrost Tunnel CGPs Iteration 2. Here it is possible to see the distribution of the error.

Permafrost Tunnel Iteration 3 - Class: Ground

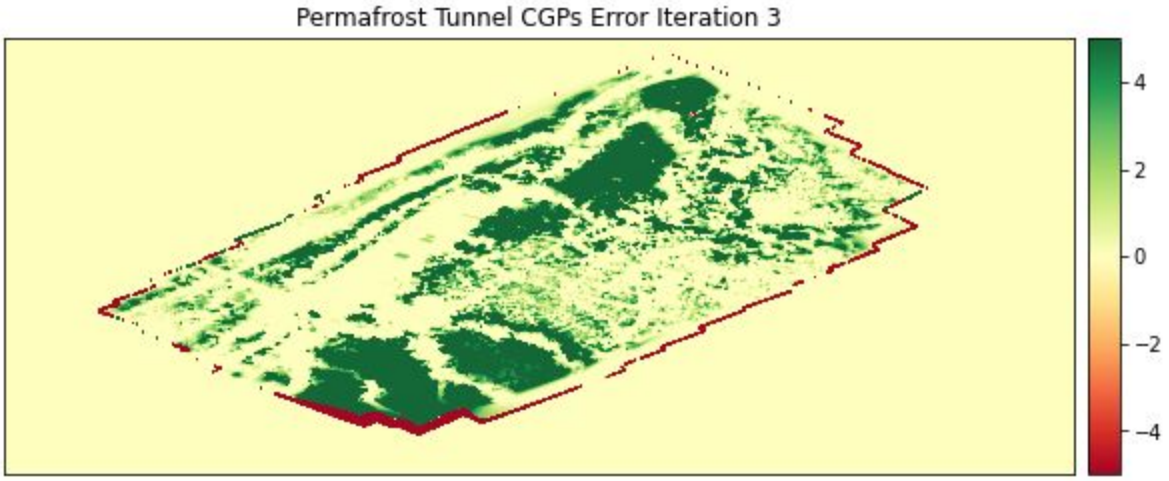

Figure 18: This is a differencing of a digital terrain produced with the ground classification settings “Class: Ground” and the baseline default settings “Class: Any Class”. The areas in red illustrate negative elevation changes in the model in meters, while the areas in green illustrate positive elevation changes in meters.

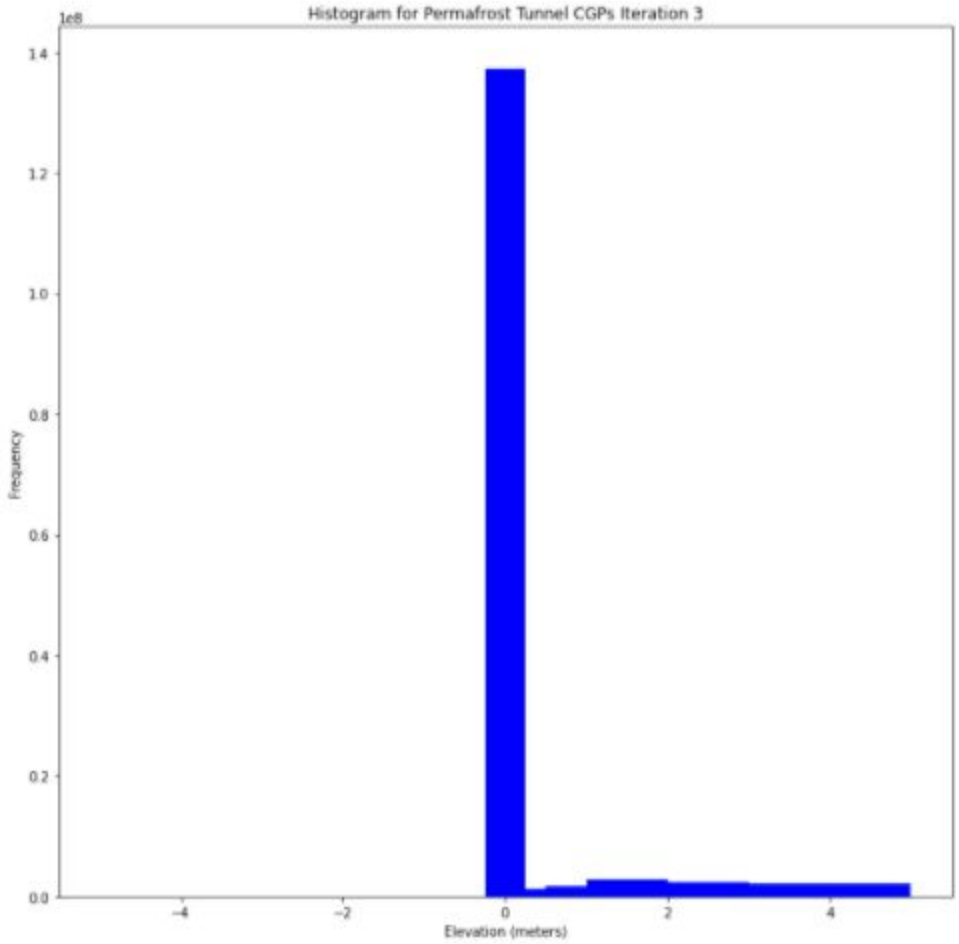

Figure 19: This is a histogram of the Permafrost Tunnel CGPs Iteration 3. Here it is possible to see the distribution of the error.

Permafrost Tunnel Iteration 4 - Class: Low Vegetation

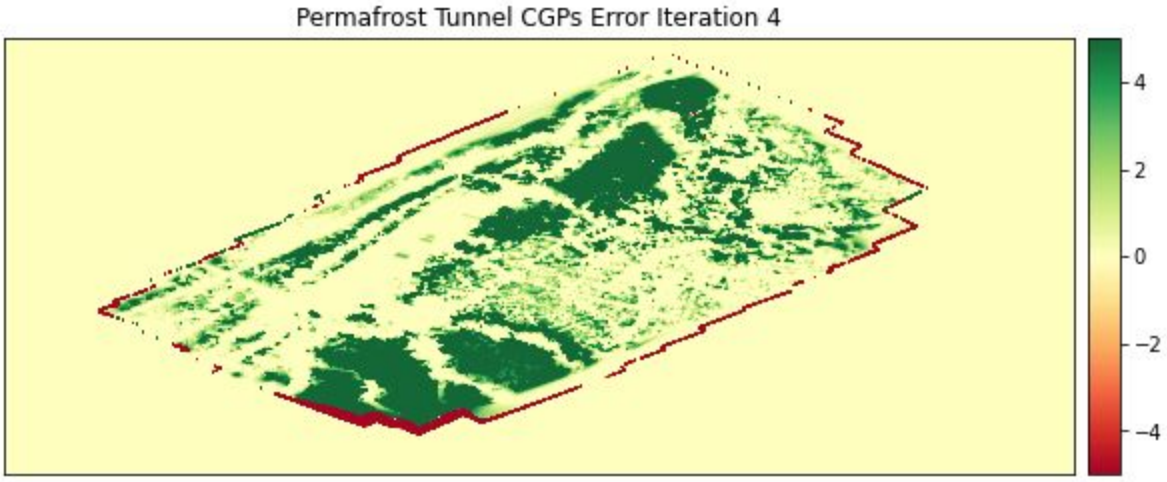

Figure 20: This is a differencing of a digital terrain produced with the ground classification settings “Class: Low Vegetation” and the baseline default settings “Class: Any Class”. The areas in red illustrate negative elevation changes in the model in meters, while the areas in green illustrate positive elevation changes in meters.

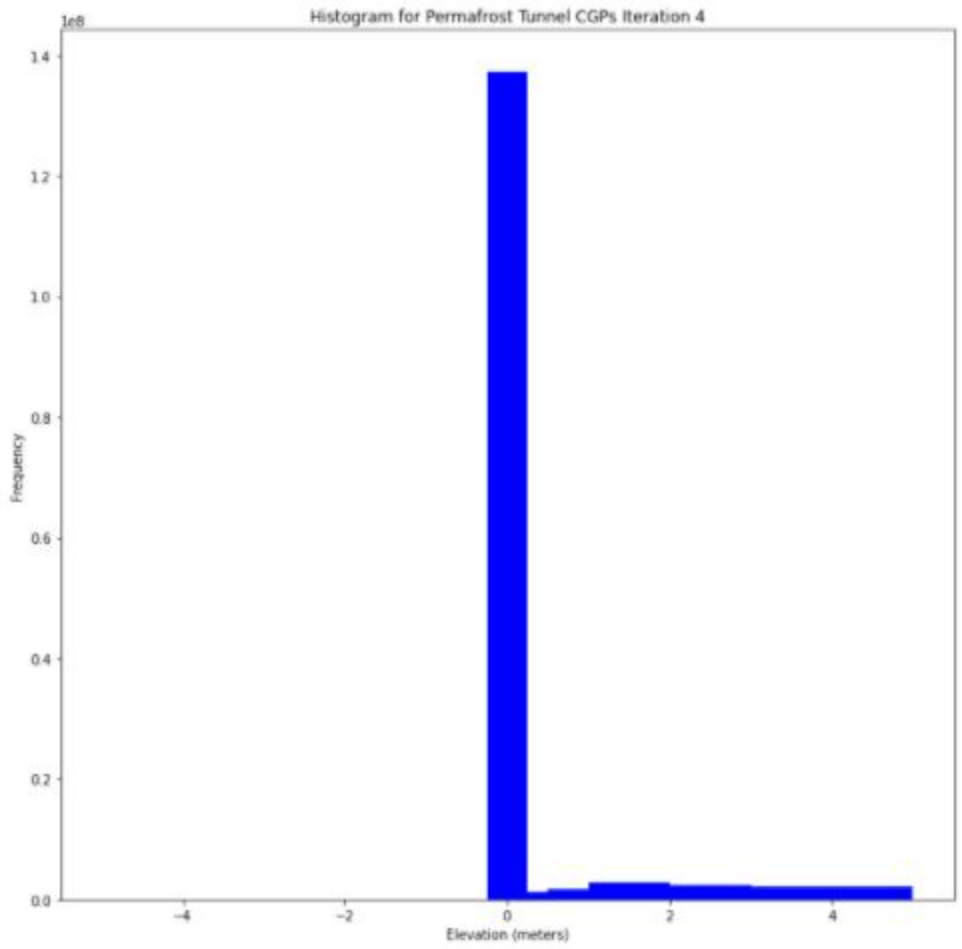

Figure 21: This is a histogram of the Permafrost Tunnel CGPs Iteration 4. Here it is possible to see the distribution of the error.

These iterations show that there is a lot of potential for variance in models due to the different classifications of ground points. Further iterations to explore these settings will need to be conducted in order to fully optimize the processing.

Recommendations

When processing sites, exclusively using GCPs with errors less than 0.1 meters would be optimal. Having this standard will allow for future comparisons of the same sites to be more meaningful. Changes in the topography will not become convoluted by error margins. This will in turn allow for more receptive analysis and more accurate models.

For the optimization of ground point classification, future iterations that test class, max angle, max distance, and cell size will need to be conducted. The individual impact of each of these settings will need to be looked at, as well as their potential to impact on other respective settings. Additionally, several sites should be tested with these iterations to test how well the settings carry over.

Acknowledgements

I would like to thank the Engineer Research and Development Center for funding this project. I would also like to thank the Alaska Center for Energy and Power's Utility Internship that has provided me with the opportunity to work on this project as well as contributing many resources to facilitate learning. I would like to thank my mentor, Erin Trochim, for her guidance and patience; I could not have done it without her. I would like to thank Bob Torgerson for his persistence in helping me with technical difficulties. I would also like to thank Heike Merkel and Patty Eagan for their unrelenting support and positivity.

References

Westoby, M. J., Brasington, J., Glasser, N. F., Hambrey, M. J., & Reynolds, J. M. (2012). 'Structure-from-Motion' photogrammetry: A low-cost, effective tool for geoscience applications. *Geomorphology*, *179*, 300–314. https://doi.org/10.1016/j.geomorph.2012.08.021

Remondino, F. (2011). UAV PHOTOGRAMMETRY FOR MAPPING AND 3D MODELING – CURRENT STATUS AND FUTURE PERSPECTIVES –https://d1wqtxts1xzle7.cloudfront.net/42061328/UAV_PHOTOGRAMMETRY_FOR_MAPPING_AND_3D_MO20160204-20906-t6geeb.pdf?1454605285=&response-content-disposition=inline%3B+filename%3DUAV_PHOTOGRAMMETRY_FOR_MAPPING_AND_3D_MO.pdf&Expires=1596782560&Signature=QCK3M~maizQVT6fYxtXvdYkd0~2x1CcaqMV921i~h6l356cvF1wghshd9qqcmne4doLdMUFV8IQn2KsJg0XKLbFqK93h6sqEg-ZoRZI5xvpWMEoFHQYqJRlM2YOivDf9Iw2YcLu8PvLe2cjMbQcip6DTOGZ14zxEfpUhAaHwkDmlW0vyAF-AiVGtFTcYhhQCmWf47ncSuFDSNJs6iGclMat47o3sWBtu2iOJAXTDYK-vrY2i1A-Ez5GyfIGbVcTivBSgYyui23gmT4AyOEkDC7yKrKaecQZKjAcIAMvvWbt9YBenV0JWgyNo1MeNIctYwrVexVgNjf5c3Y3GbOo0Ng__&Key-Pair-Id=APKAJLOHF5GGSLRBV4ZA.